A Dual-Band Dual-Polarized 2x2 Antenna array with beamforming for 5G AiP and mmWave Applications

Sheng-Chi Hsieh
Cetral Reserch and Development
ASE Gruop
Kaohsiung, Taiwan
Rick_Hsieh@aseglobal.com

Hong-Sheng Huang
Cetral Reserch and Development
ASE Gruop
Kaohsiung, Taiwan
SamHS_Huang@aseglobal.com

Wen-Chun Hsiao
Cetral Reserch and Development
ASE Gruop
Kaohsiung, Taiwan
Stanley_Hsiao@aseglobal.com

Cheng-Yu Ho
Cetral Reserch and Development
ASE Gruop
Kaohsiung, Taiwan
Derk_Ho@aseglobal.com

Chen-Chao Wang
Cetral Reserch and Development
ASE Gruop
Kaohsiung, Taiwan
Alexcc_Wang@aseglobal.com

***Abstract*—In this study, we present a dual-band (28/39GHz) 2 by 2 antenna array design on a 10(4+2+4) multi-layer organic substrate with broad bandwidth and higher isolation onto a compact AiP module. In addition, the H-type slot antenna structure can improve interference and isolation between 28 and 39GHz bands. The measured result shows the isolation can larger than 15dB between low and high band. For antenna measurement, the spherical of probing chamber is utilized to validate 28/39GHz antenna pattern and performance with a package level passive testing. Our AiP measured result shows the return loss is better than 10 dB in 23.5-30.5 GHz range, with ~7 GHz bandwidth and provides a high-gain per element (above ~6 dBi) radiation pattern for 28GHz applications. For 39GHz band, the antenna has 7 GHz bandwidth and provides a 5 dBi gain between 38-45 GHz. Comparison of S-parameter between simulated and measured results, there is a good correlation to obtain the quality of manufacturing. Furthermore, a 28GHz beamforming array is designed and demonstrated. The beamfoming array consists of a four-channel transceiver with 2 x 2 antenna array. The beamformer IC is implemented by TSMC 90-nm CMOS technology and the flip-chip bonded on BT substrate. For beamforming test, an integrated socket and load board are designed for support the mmWave module and then connection between DUT and test system. The load board substrate includes the IF, LO, and DC distribution network for respectively. There are 4-channel transmit beamforming array front-end module for testing. Finally, the 3D beam steering of 2 by 2 antenna array is measured with multi-states at 28 GHz, with a maximum realized gain of 11.8 dBi achieved in the main beam (θ=0°). It shows that beamforming can be generated at a specific beam direction by controlling the phase of the signal in each antenna element.**

Keywords—Antenna in package(AiP), Dual-band Antenna, mmWave Antenna, Broad band antenna

I. INTRODUCTION

The new radio (NR) frequency bands of 5G communication are distributed in two defined frequency ranges (FR), which are FR1: 450 MHz to 6 GHz and FR2: 24.25 GHz to 52.6 GHz [1]. There are three dimensions to improve the performances, which are massive IOT, low latency, and the enhanced mobile broadband (eMBB), for the usage of massive connectivity, ultra-high reliable and low latency, and capacity enhancement, respectively. As shown in Fig. 1, the physical wavelengths for mmWave range are about one to ten millimeters so that the antenna size in the millimeter-wave band is obviously small to design into package. The antenna in package (AiP) technology is applied to satisfy electronic devices of the fifth generation(5G) communication nowadays in the millimeter-wave range. Recently, mmWave frequency range is widely discussed and expected to provide higher capability of handling larger data volume and higher speed for the 5G and beyond 5G(B5G) wireless communications. The technology trend shows a strong demand for a larger bandwidth (BW), multi-band, low cost materials into antenna in package technology (AiP) [2-3]. Compared with glass substrate [4], low-temperature co-fired ceramic (LTCC) [5], on-chip [6] or organic substrate [7] fabrication technologies, the BT-based organic substrate is a relatively cost-effective solution. Although some mmW AiP studies are demonstrated on the BT-based substrates applications. However, the multi-frequency bands are a key issue when a lot of the antennas designed onto a one package. In this work, a compact size of dual-band 2 by 2 antenna array on 10(4+2+4) multi-layer organic substrate that achieves broad bandwidth and higher isolation on a 13 mm x 13 mm AiP module.

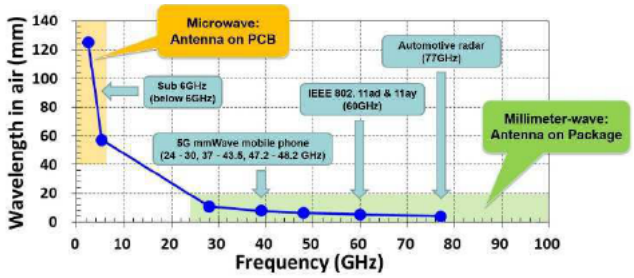

Fig. 1. Comparison of wavelength in air at microwave band and millimeter-wave band.

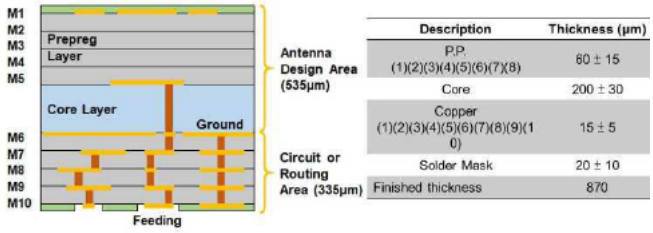

Description	Thickness (μm)
P.P. (1)(2)(3)(4)(5)(6)(7)(8)	60 ± 15
Core	200 ± 30
Copper (1)(2)(3)(4)(5)(6)(7)(8)(9)(10)	15 ± 5
Solder Mask	20 ± 10
Finished thickness	870

Fig. 2. The cross-section view of the AiP stack-up structure.

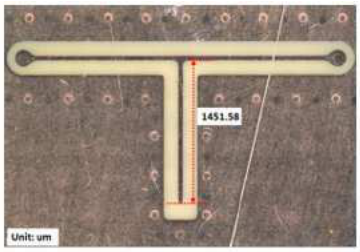

(a) T-resonator

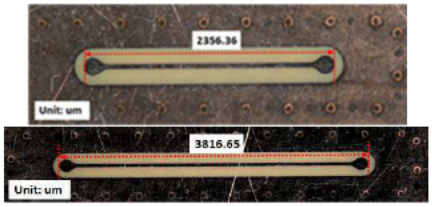

(b) Microstrip transmission line

Fig. 3. The test kits are implemented on 4+2+4 multi-layer substrate. (a) T-resonator, (b) Microstrip transmission line TL1 and TL2

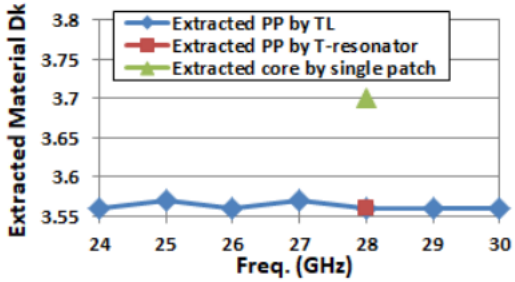

Fig. 4. The extracted material characteristic of 4+2+4 multi-layer substrate by designed test kits.

II. Antenna Design

A. Extracted Material Property

The stack up of 10 layers (4+2+4) with low Dk and Df of core/pregrep(p.p) is shown in Fig. 2. The BT and core material are GHPL970LF and CCL-HL972LF respectively. Two 50-Ω microstrip lines with different trace length are employed to extract the material property. After applying multimode TRL calibration, the probe pad and the transition taper effect are eliminated and resulting in a simple transmission line model with a 15 mm length difference between the long and the short lines. The relationship between the effective relative permittivity (ε_{eff}) and the phase constant (β) of a microstrip line is shown as below:

$$\frac{c}{\sqrt{\varepsilon_{eff}}} = \frac{\omega}{\beta} \tag{1}$$

where c is the speed of light in vacuum and ω is the angular frequency. ε_{eff} is obtained from the measured phase of S_{21} by (1), then the relative permittivity (ε_r) of the material is converted by the following equation [8] for $W/h \geq 1$:

$$\varepsilon_{eff} = \frac{\varepsilon_r + 1}{2} + \frac{\varepsilon_r - 1}{2}\left(1 + \frac{12h}{W}\right)^{-\frac{1}{2}} \tag{2}$$

where W is the width of the microstrip line and h is the thickness of the substrate.

As shown in Fig. 3, the designed T-resonator and microstrip transmission lines are used to extract the material characteristic of 4+2+4 multi-layer substrate. The extracted material characteristic of 4+2+4 multi-layer substrate are shown in Fig. 4.

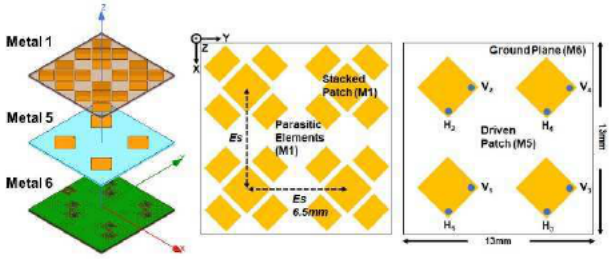

Fig. 5. Geometry of the 2 by 2 antenna

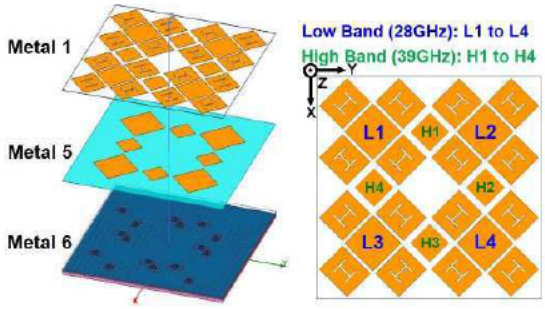

Fig. 6. Geometry of the dual-band antenna

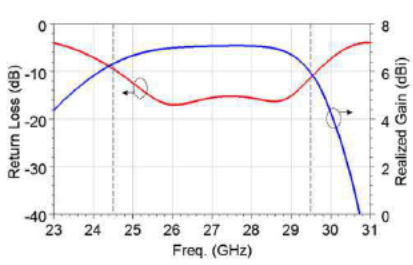

(a)

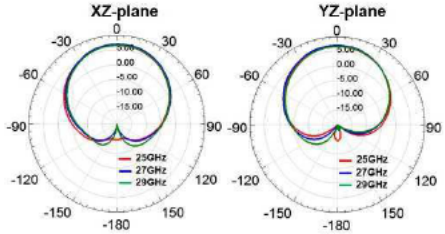

(b)

Fig. 7. The simulated result for low band antenna (a) return loss and realized gain (b)2D pattern for XZ-plane and YZ-plane at 25GHz, 27GHz, and 29GHz.

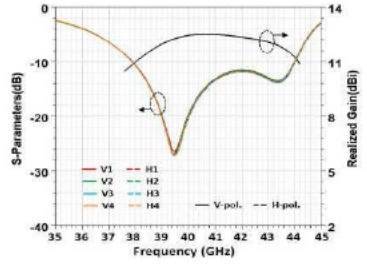

(a)

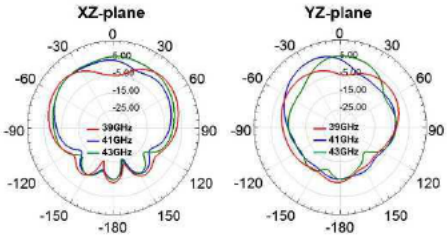

(b)

Fig. 8. The simulated result for high band antenna (a) return loss and realized gain (b)2D pattern for XZ-plane and YZ-plane at 39GHz, 41GHz, and 43GHz.

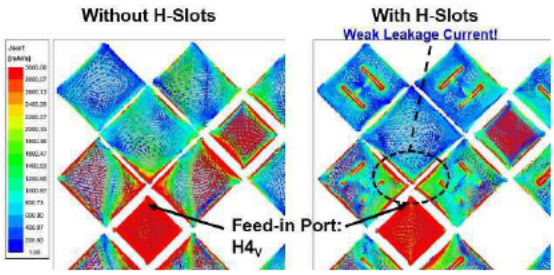

(a)

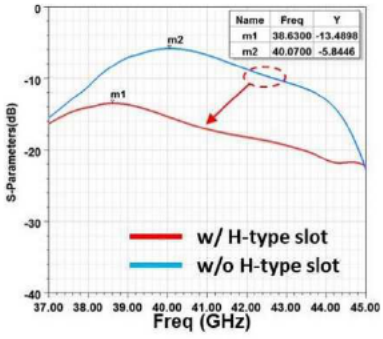

(b)

Fig. 9. The EM simulation of dual band antenna (a) current distributions (b) The isloation with and withoiut H-slot

B. *Dual-Band Antenna Design*

The Dual-Band antenna design is based on a stacking patch antenna with parasitic structure. In order to improve the performance of patch antenna, the stacking patch antenna with parasitic elements has advantages of wider bandwidth and higher antenna gain. For transmitting performances, this features improve the beam scanning range and array gain, which will enhance the transmission quality while beamforming. On the antenna design, the driven patch is printed on the Copper 5 layer and coupled to the stacked patch which is printed on the Copper 1 layer. The parasitic patches located close to the staked patch on the Copper 1 layer as well. The ground plane is printed on Copper 6. Fig. 5 shows the proposed 2 by 2 antenna with multi-parasitic elements, where

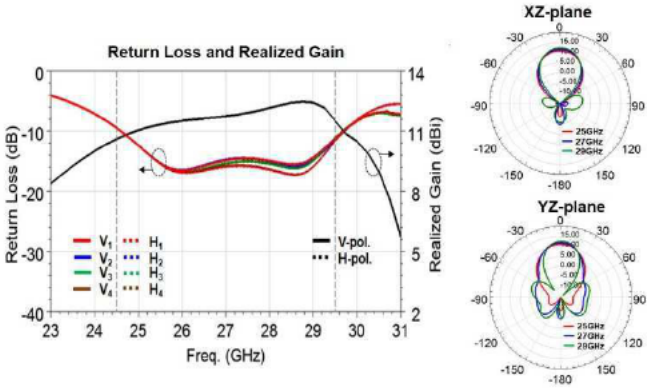

Fig. 10. The simulated 2D radiation pattern for 28GHz 2x2 antenna array

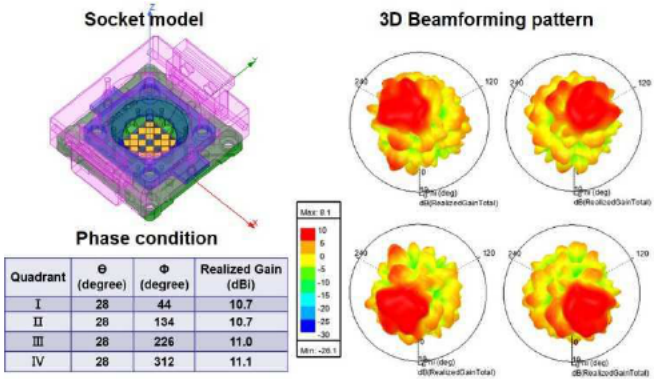

Quadrant	Θ (degree)	Φ (degree)	Realized Gain (dBi)
I	28	44	10.7
II	28	134	10.7
III	28	226	11.0
IV	28	312	11.1

Fig. 11. The simulated 3D beam steering pattern with test socket model

the multi-parasitic elements are located around the stacked patch to provide multi-modes responses. The dimension of the driven patch and staked patch with parasitic elements for maximum gain is given by half of the wavelength. The antenna can be extended to a 2 by 2 array design as adjusting the spacing between array elements. In order to obtain the best directivity and linearity, the linear arrays are designed to have half-wave spacings to give identical results. The spacing between the elements is optimized to 6.5mm. The 2x2 antenna array consists of four antenna elements with two feeding ports placed orthogonally in each antenna element for dual-polarization. Its dimension is 13 x 13 x 0.87 mm^3. For 39 GHz antenna design, the construction of antenna is a stacked patch antenna as well. It is embedded and placed between 28GHz elements with the same ground plane to combine as a dual band antenna with different input feeding. Fig. 6 presents the geometry of the proposed dual band 28/39 GHz antenna. Fig. 7 and Fig. 8 show the simulated return loss and 2D radiation pattern for low band and high band antenna. In this work, we add a H-slot to a patch antenna which enables it to adjust current distributions and improve isolation between two bands of antennas. Fig. 9(a) shows the surface current distributions of the dual band antenna with H-slot. The isolation is effectively improved from 5dB to 15dB as shown in Fig. 9(b).

C. *Beamforming Simulation with Test Socket*

In order to drive 2x2 antenna array for beamforming generation at the desired XZ and YZ directions, each antenna of array must have an appropriate phase difference with respect to its adjacent antenna where θ and Φ denote the relative phase difference between the antenna located in the XZ and YZ directions. For the beamforming performance, the simulated 2D radiation patterns of the V-pol are presented in the XZ- and YZ- planes at 25GHz, 27GHz, and 29GHz,

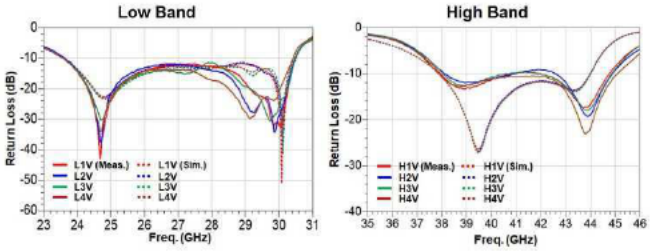

Fig. 12. Simulated and measured return loss

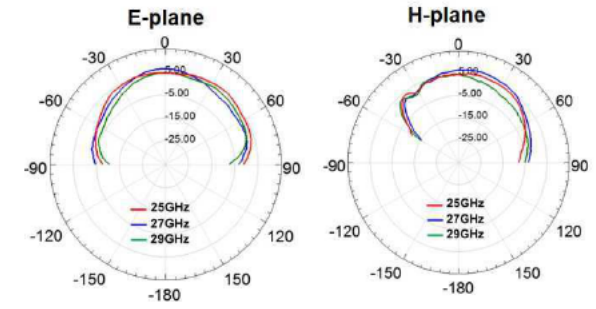

(a)

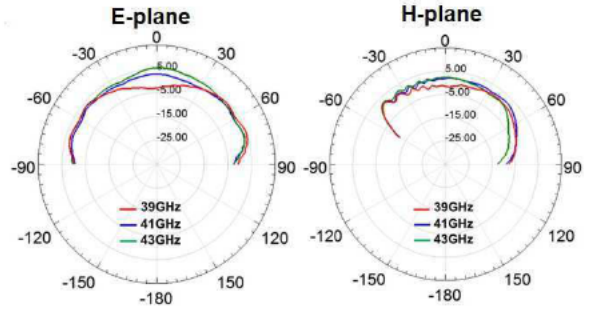

(b)

Fig. 13. The measured peak gain and 2D radiation pattern(a) Low band (b) High band

respectively, as shown in Fig. 10. It is essential to obtain the 3D beam steering pattern to ensure the radiation performance with phased antenna array that can be integrated with a beamformer circuit for active test in the chamber. In Fig. 11, the 3D beam steering is simulated in all four quadrants at 28GHz. The simulated model is not only 2x2 antenna array but also include the test socket for performance evaluation with a real test in the chamber. The simulation shows the maximum realized gain of 11.1dBi is achieved in the beam direction (θ=28°, Φ=312°) of quadrant IV, and shows the beamforming can work properly by controlling the phase of signal in each antenna element.

III. Measurement Result

In this section, the beamformer IC and setup are firstly introduced. And then the simulated and measured results for the return loss, bandwidth, peak gain and the radiation patterns are presented and compared. The AUT is measured in an far field and a spherical of probing chamber that the AUT is placed on a low permittivity foam and measured by probing. Fig. 12 shows the measured and simulated return loss of the each elements for 2 by 2 antenna array. The results show our AiP design has better than 10 dB return loss in 23.5-30.5 GHz range, with ~7 GHz bandwidth for 28GHz band antenna. For 39GHz band antenna, the antenna has 7GHz bandwidth from 38-45 GHz. The measurement result demonstrates a good

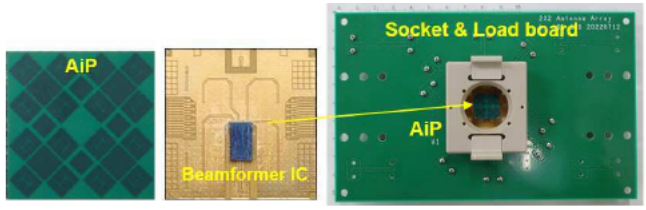

Fig. 14. The photographs of the fabricated AiP and socket

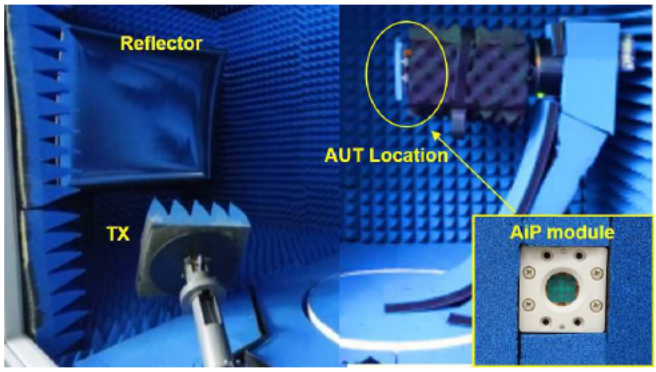

Fig. 15. mmWave AiP measurment setup in CATR chamber

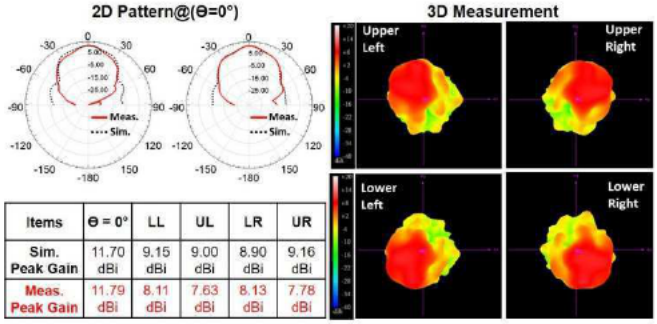

Items	Θ = 0°	LL	UL	LR	UR
Sim. Peak Gain	11.70 dBi	9.15 dBi	9.00 dBi	8.90 dBi	9.16 dBi
Meas. Peak Gain	11.79 dBi	8.11 dBi	7.63 dBi	8.13 dBi	7.78 dBi

Fig. 16. The measured 2D & 3D beam steering pattern in CATR chamber

agreement with simulation. Fig. 13 shows the measured gain pattern and peak gain for low band and high band antenna. The measured peak gain is about 6 dBi and 5dBi for low band and high band antennas, respectively.

For beamforming test, the beamformer IC can be flip-chip bonded on the BT substrate, combined with the antenna array. The beamformer IC is implemented by TSMC 90-nm CMOS technology. It is composed of one-way 4x4 Butler matrix, four LNA (low noise Amplifier), two VGA (Variable Gain path Selector), one Coupler and one SPDT Switch. Since the whole beamformer contains 4x4 Butler matrices, the circuit size of the single Butler matrix must be considerable minimized. The Chip size is 2.97x1.75mm^2. Fig. 14 shows the photographs of the fabricated AiP with a beamformer IC and test socket on load-board for beamforming test. The simulated progressive phase differences between the adjacent port are $45^0 \pm 5^0$. The overall integrated 2x2 AiP is measured by CATR chamber (Compact Antenna Test Range), as shown in Fig. 15. The AiP module can be mount in the test socket. The absorbers are placed around the module to avoid the holder scattering. All the setups and acquired data are integrated on a measurement panel programming by NI LabVIEW. The calibration phases for each channels needed before beamforming measurement. Then, the circuit calibration and the realized gain calibration have to correct. Once the calibration is done, the beam performance are obtained. The measurement of beam steering

in all four quadrants at 28GHz, the maximum realized gain of 11.8 dBi is achieved in the main beam (θ=0°). The 3D beam steering is measured in all four quadrants at 28GHz as shown in Fig. 16.

IV. Conclusions

This paper demonstrates a 2x2 dual-band antenna array using 4+2+4 multi-layer buildup substrates for 5G mmWave applications. As a result, our stacked patch antenna with parasitic elements achieves broadband operation. The proposed 2 by 2 dual-band antenna exhibits a 7 GHz bandwidth with a 6 dBi peak gain per element within the 23.5-30.5 GHz for low band. For 39GHz band, the antenna has 7 GHz bandwidth and provides a 5 dBi gain per element from 38-45 GHz. In addition, we design the H-type slot structures onto antenna that it can improve interference and isolation between 28 and 39GHz bands. The measured result shows the isolation can larger than 15dB between low and high band. We also measured beam steering by controlling the phase of each element, which ensures that the phased array is working properly. The 3D beam steering of 2 by 2 antenna array is presented with multi-states at 28 GHz, with a maximum realized gain of 11.8 dBi achieved in the main beam (θ=30°).

Acknowledgment

The authors would like to acknowledge National Chung Cheng University, Lab543, Professor Chang for technical support to overcome a lot of testing issues, and successfully realize the proposed beamforming test.

References

[1] 3GPP, "User Equipment (UE) radio transmission and reception; Part 1: Range 1 Standalone (Release 15)." Tech. rep vol. 3GPP TS 38.101-1 V1.0.0: NR, Dec. 2017.

[2] Y. Zhang and J. Mao, "An Overview of the Development of Antenna-in-Package Technology for Highly Integrated Wireless Devices," in *Proceedings of the IEEE*, vol. 107, no. 11, pp. 2265-2280, Nov. 2019.

[3] A. Fischer, Z. Tong, A. Hamidipour, L. Maurer and A. Atelzer, "77-GHz Multi-Channel Radar Transceiver With Antenna in Package," IEEE *Trans Antennas Propag.*, vol. 62, no. 3, pp. 1386 – 1394, March 2014.

[4] K. -Q. Huang and M. Swaminathan, "Antennas in Glass Interposer for sub-THz Applications," *in Proc. IEEE 71st Electron. Compon. Technol.Conf. (ECTC)*, pp. 1150-1155, 2021.

[5] R. Kulke et al., "24 GHz radar sensor integrates patch antenna and frontend module in single multilayer LTCC substrate," in Proc. *Eur. Microelectronics and Packaging Conf.*, Jun. 2005, pp. 239–242.

[6] X. Gu, D. Liu, and B. Sadhu, "Packaging and antenna integration for silicon-based millimeter-wave phased arrays: 5g and beyond," *IEEE Journal of Microwaves*, vol. 1, no. 1, pp. 123-134, 2021.

[7] S. -C. Hsieh, F. -C. Chu, C. -Y. Ho, W. -Y. Chen and C. -C. Wang, "mmWave AiP Measurement Turnkey Solution in Millimeter-Wave Wireless Communication Applications," 2*020 IEEE 70th Electronic Components and Technology Conference (ECTC),* pp. 114-119, 2020.

[8] I. J. Bahl and R. Garg, "A designer's guide to stripline circuits," Microwaves, pp. 90–96, Jan. 1978.